Appropriate sagittal positioning of femoral components in total knee arthroplasty to prevent fracture and loosening

a finite element study

From The Second Hospital of Jilin University, Changchun, China

Cite this article:
Bone Joint Res 2024;13(10): 611–621.

DOI: 10.1302/2046-3758.1310.BJR-2023-0362.R2

Correspondence should be sent to Jincheng Wang
jinchengwangjlu@163.com

Q. Wan,[1] Q. Han,[1] Y. Liu,[1] H. Chen,[1] A. Zhang,[1] X. Zhao,[2] J. Wang[1]

[1]Department of Orthopedics, The Second Hospital of Jilin University, Changchun, China
[2]Department of Endocrinology and Metabolism, The First Hospital of Jilin University, Changchun, China

Aims
This study aimed to investigate the optimal sagittal positioning of the uncemented femoral component in total knee arthroplasty to minimize the risk of aseptic loosening and periprosthetic fracture.

Methods
Ten different sagittal placements of the femoral component, ranging from -5 mm (causing anterior notch) to +4 mm (causing anterior gap), were analyzed using finite element analysis. Both gait and squat loading conditions were simulated, and Von Mises stress and interface micromotion were evaluated to assess fracture and loosening risk.

Results
During gait, varied sagittal positioning did not lead to excessive Von Mises stress or micromotion. However, under squat conditions, posterior positioning (-4 and -5 mm) resulted in stress exceeding 150 MPa at the femoral notch, indicating potential fracture risk. Conversely, +1 mm and 0 mm sagittal positions demonstrated minimal interface micromotion.

Conclusion
Slightly anterior sagittal positioning (+1 mm) or neutral positioning (0 mm) effectively reduced stress concentration at the femoral notch and minimized interface micromotion. Thus, these positions are deemed suitable to decrease the risk of aseptic loosening and periprosthetic femoral fracture.

Introduction
Despite a high ten- to 15-year survival rate exceeding 90% for total knee arthroplasty (TKA),[1] the occurrence of postoperative complications remains a challenge.[2] Periprosthetic fracture and aseptic loosening are severe and common complications after TKA, accounting for 2.6% and 29.6% of all revision surgeries, respectively.[3,4] Several clinical studies and mechanical assessments have underscored the heightened risk of periprosthetic fracture associated with anterior femoral notching resulting from improper osteotomy.[5-8] Consequently, there is a consensus among joint surgeons on the importance of minimizing the creation of an anterior femoral notch during TKA. Despite this consensus, the occurrence of femoral anterior notching remains notable in clinical practice, with reported incidence rates ranging from 3.5% to 29.8%. The advent of computer navigation technology has considerably improved the precision of the coronal alignment of the femoral component during TKA.[9,10] However, challenges persist in achieving reliable sagittal positioning of the femoral component due to uncertainties surrounding the distal femoral reference

Bone & Joint Research

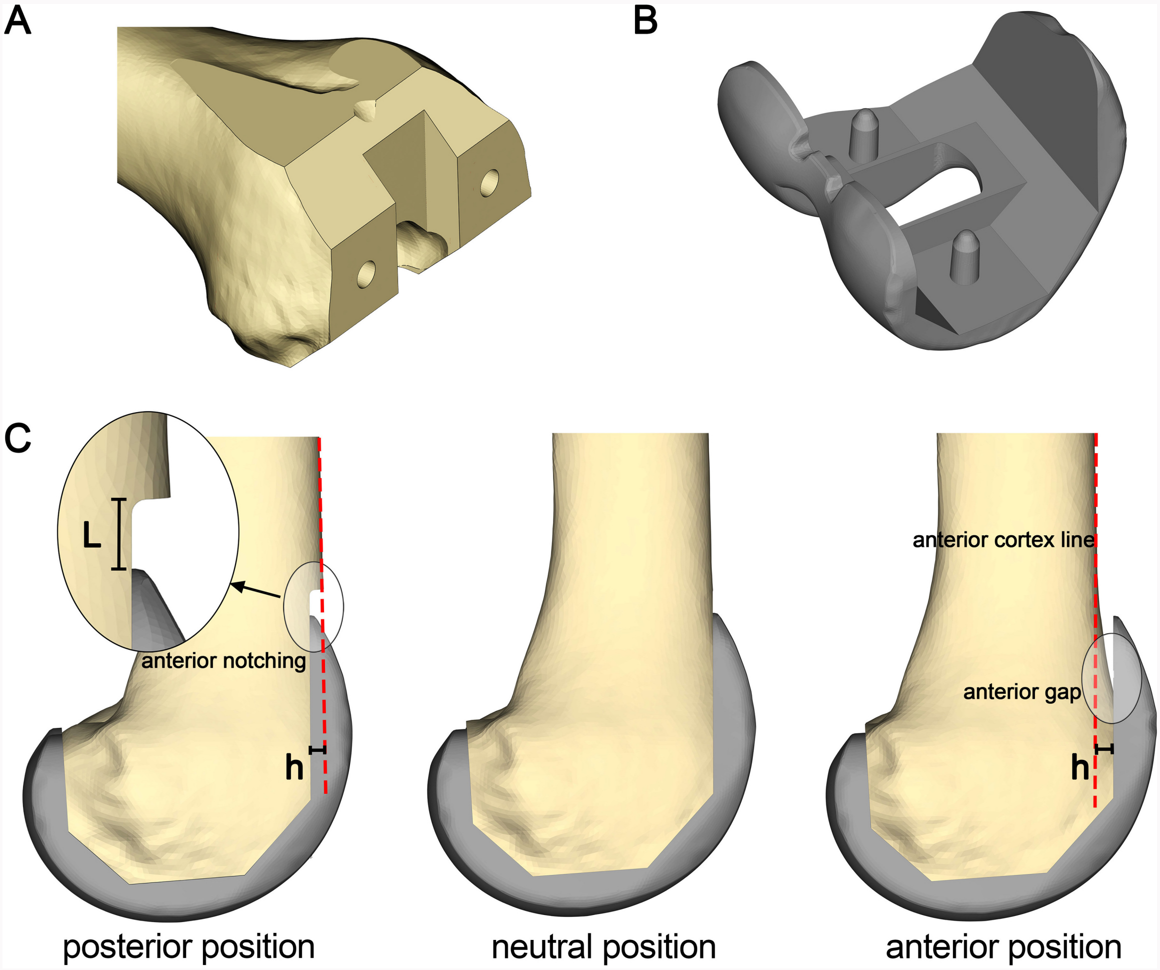

Fig. 1

Illustration of finite element analysis models and different sagittal positioning of the femoral component. a) The femur model. b) The femoral component of the high flexion posterior stable prosthesis. c) Different sagittal positioning of the femoral component. The anterior positioning causes a gap, and the posterior positioning causes a notch. 'L' represents the distance between the anterior flange of the femoral component and the notch, and 'h' represents the sagittal position of the femoral component.

point.[11,12] This sagittal positioning can be categorized as anterior, neutral, or posterior relative to the anterior cortex line (Figure 1c), with posterior positioning potentially leading to anterior femoral notching. Interestingly, studies have indicated that the use of computer navigation may inadvertently increase the likelihood of creating an anterior femoral notch.[13,14]

In cases where an anterior femoral notch occurs intraoperatively due to poor sagittal positioning, a salvage intramedullary stem can be employed for corrective measures to alleviate stress concentration resulting from the notch.[15] In such instances, it is crucial to have guidance in determining the critical depth of the femoral notch necessitating the use of a salvage intramedullary stem to mitigate the risk of periprosthetic fracture under the physiological loads associated with daily activities. Presently, research lacks clarity on the relationship between the depth of the femoral notch and the risk of periprosthetic fracture. Some clinical studies have reported contradictory findings,[7,16,17] while existing biomechanical tests and finite element analyses (FEAs) have been conducted under simplified loading conditions.[6,8] There is a need for insight into outcomes under loading conditions that more accurately reflect the physiological environment.

In addition to periprosthetic fractures, aseptic loosening is a common complication following TKA. Cemented fixation results in stable initial fixation, yet the incidence of aseptic loosening tends to rise over prolonged use of the prosthesis.[18] Conversely, advancements in prosthesis design, coupled with the development of microporous and coated surfaces,[19,20] have led to lower rates of long-term aseptic loosening with uncemented fixation, which fosters robust biological fixation once initial stability is achieved.[18,21] As the average age of TKA patients decreases and life expectancy increases, the demand for long-term or lifelong prosthetic usage intensifies, rekindling interest in uncemented fixed prostheses.[22] In this context, achieving initial stability is pivotal with uncemented prostheses, as it lays the foundation for strong biological fixation. Improper sagittal positioning may compromise the stability of the femoral component due to inadequate gap tightness and contact area between the prosthesis and the femoral anterior/posterior condyle (Figure 1c), leading to initial instability.[23] However, the influence of the sagittal positioning on the stability of the femoral component remains largely unexplored. Thus, further research is imperative to comprehend the biomechanical effects of

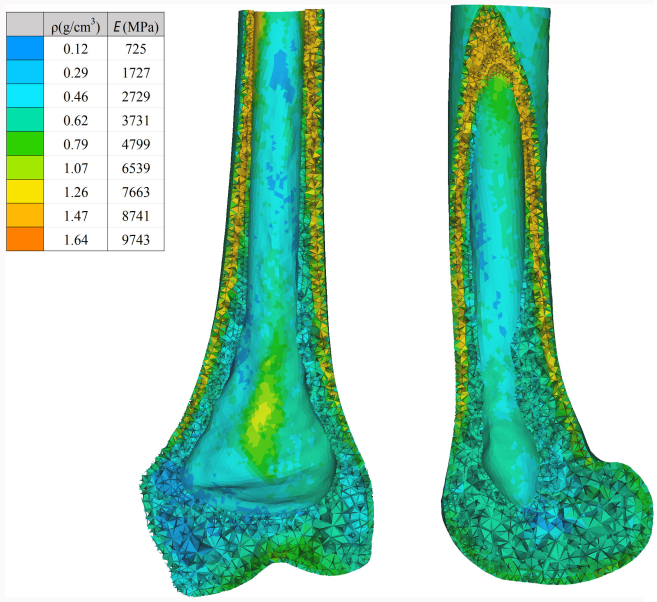

Fig. 2
Material distribution and meshing of the femur model (coronal and sagittal sections).

femoral component sagittal positioning on the risk of aseptic loosening.

In this study, our objective was to investigate the biomechanically appropriate sagittal positioning of the femoral component in TKA to mitigate the risk of fracture and loosening. Given the challenge of replicating the intricate biomechanical conditions within the joint using mechanical testing machines, we employed FEA to assess the Von Mises stress distribution within the femur under two prevalent loading conditions: gait and squat. We examined the squat loading scenario due to reported instances where excessively posterior sagittal positioning led to anterior full-thickness cortical notching, significantly reducing femoral bending strength.[6]

Our evaluation focused on assessing the risk of bone fracture and aseptic prosthesis loosening across various femoral sagittal positioning configurations. We hypothesized that the neutral position represents the most suitable sagittal positioning for the femoral component.

Methods

Inhomogeneous 3D femur remodelling and surgical simulation

A 3D femur model was reconstructed based on CT scan data (Philips iCT 256 CT scanner at 120 kVp and 156 mA with a slice thickness of 0.602 mm; Royal Philips, Netherlands) obtained from a 22-year-old female volunteer who was recruited through community outreach efforts (Figure 1a). The CT scan data were processed using Mimics 21.0 software (Materialise, Belgium) for the femur modelling. The femoral component used was a high flexion posterior stable A3 series prosthesis (AK Medical, China). This choice was made because posterior stable prostheses typically result in a greater flexion gap compared to the extension gap after resection of the posterior cruciate ligament. Adding a distal femoral osteotomy or posterior displacement of the femoral prosthesis can increase the risk of anterior notching.[24] Point cloud data obtained from a 3D scanner were imported into Geomagic Designx 2019 software (3D Systems, USA) for reverse modelling (Figure 1b). Each femur was sectioned at the middle of the diaphysis (242 mm from the distal femur's surface), which was consistent with previous FEA[25,26] and experimental studies.[27,28] The surgical simulation was conducted under the guidance of experienced surgeons JW and QH. The rotational positioning of the prosthesis was referenced to the surgical transepicondylar axis, while the flexion/extension positioning was referenced to the anterior cortical line. As depicted in Figure 1c, at least one study has validated that the most suitable sagittal flexion/extension position for femoral prostheses is perpendicular to the anterior cortex line, typically around 3° to 5° of flexion relative to the mechanical axis.[29] Therefore, the anterior femoral resection plane was aligned parallel to the anterior cortex line, serving as the baseline and labelled as 0 mm. The sagittal position of the femoral component, denoted as "h", ranged from -5 to +4 mm, representing 'posterior position (-5 to -1 mm)', 'neutral position (0 mm)', and 'anterior position (+1 to +4 mm)'. For example, a sagittal position of -3 mm meant that the depth of the anterior femoral notching was 3 mm. 'L' represented the distance between the anterior flange of the femoral component and the notch (Figure 1c). Both 1 mm and 5 mm distances were evaluated.

Based on the grayscale values (GV) derived from the CT scan data, the material property of the femur was characterized as non-homogeneous using Mimics software. Density (ρ) and elastic modulus (E) were calculated using the following formulae:[30]

$$\rho\left(\frac{\mathrm{g}}{\mathrm{m}}^{3}\right) = -13.4 + 1017GV\left(\mathrm{HU}\right), \tag{1}$$

$$E\,(\mathrm{Pa}) = -388.8 + 5925\rho\left(\frac{\mathrm{g}}{\mathrm{m}}^{3}\right). \tag{2}$$

The femur was divided into nine different materials, and the Poisson's ratio was set to 0.3 (Figure 2).[31,32] The material of the femoral prosthesis was Ti6Al4V, with an elastic modulus of 110,000 MPa and Poisson's ratio of 0.3.[33] Both bone and prosthesis materials were assumed to be linear elastic.

Meshing and boundary conditions

All models underwent discretization in Hypermesh 2020 (Altair Engineering, USA), divided into tetrahedral meshes with an element size of 0.7 mm. The mesh refinement focused particularly on the notching area, with a mesh convergence test ensuring that further refinement resulted in a difference of no more than 5%. The details of the mesh convergence test are provided in the second part of the Supplementary Material.

The FEA was conducted using Abaqus 2021 (Dassault Systèmes, France) employing an implicit formulation. The proximal femur was fully constrained in six degrees of freedom. For the gait simulation, a dynamic simulation of the entire gait process from toe-off was executed, spanning one second. Forces and moments applied were derived from previous in vivo instrumented knee implant experiments and inverse dynamic studies,[34,35] normalized based on the volunteer's body weight. Axial (F_z), anterior-posterior (F_y), and medial-lateral (F_x) tibiofemoral contact forces were applied, along with three rotational moments: internal-external (M_z), varus-valgus (M_y), and flexion-extension (M_x) (Figure 3a). The

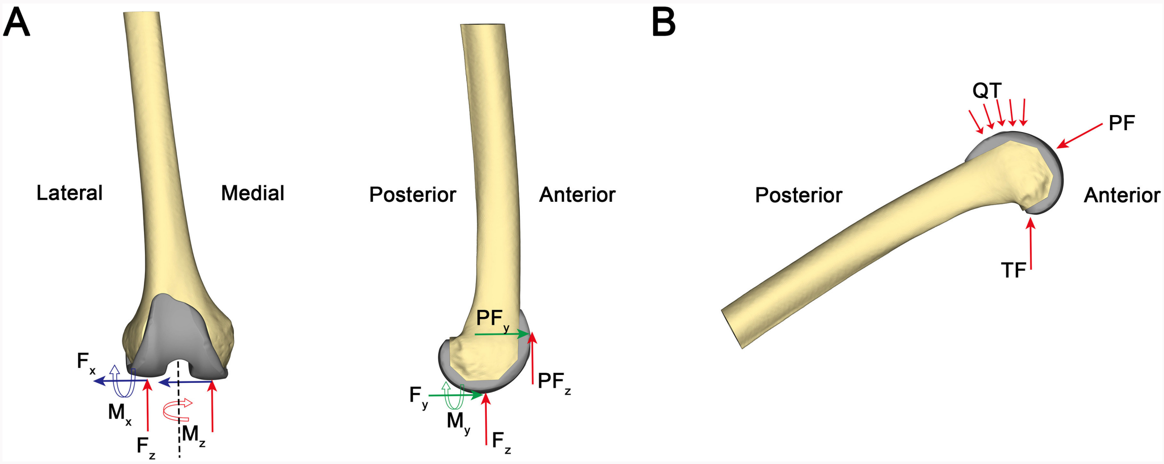

Fig. 3

Illustration of a) gait and b) squat loading conditions. Fx, Fy, and Fz represent medial-lateral, anterior-posterior, and axial tibiofemoral contact forces, respectively. Mx, My, and Mz separately mean flexion-extension, varus-valgus, and internal-external moments, respectively. PF, patella-femoral contact force; QT, quadriceps tendon forces; TF, tibiofemoral contact force.

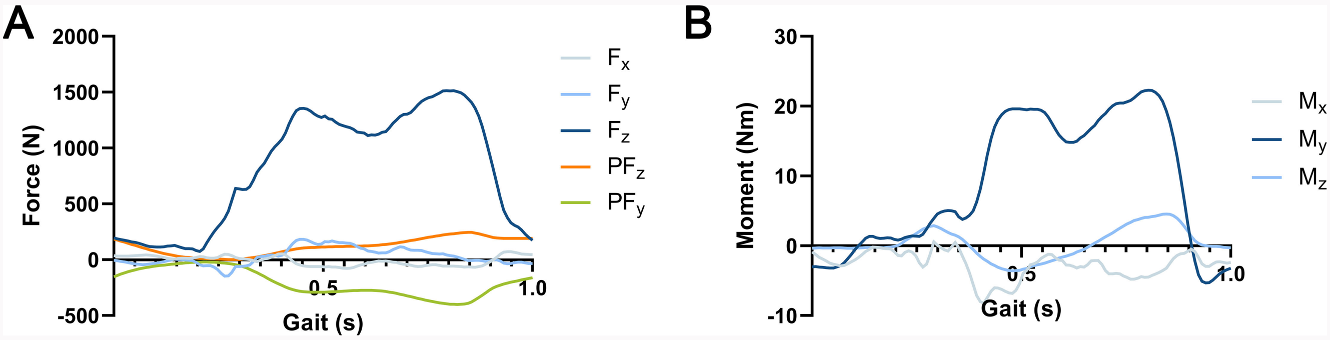

Fig. 4

a) Applied forces and b) moments on the femoral component during a whole gait cycle. The data shown in the graph are for a body weight of 60 kg.

magnitude of the applied forces and moments is illustrated in Figure 4. Notably, F_z represents the vertical force, being the primary component of the knee reaction force during gait, while M_y signifies the internal moment of the knee, significant due to unbalanced forces on the medial and lateral femoral condyles (3:2).[33] Additionally, the patellar-femoral force (PF) was considered for its significant influence on simulation results.[36]

For squat activity simulation, since there was a lack of data on the joint reaction forces and the muscle force profiles throughout the squatting process, a quasi-static analysis was conducted at 145° knee flexion, representing the maximum flexion angle of a high flexion knee prosthesis. Tibiofemoral (TF), patella-femoral (PF), and quadriceps tendon forces (QT) were set to 4.0, 7.1, and 3.6 times the bodyweight of the volunteer, respectively (Figure 3b).[35] Tibiofemoral contact forces and moments were applied to actual contact areas,[37] with the medial and lateral condyle distribution ratio set at 3:2.[38] Frictional contact was defined between the prosthesis and the bone, utilizing the Coulomb friction model with a frictional coefficient set to 0.6.[39]

Evaluation indicators and statistical analysis

In this study, two key indicators were used to assess the simulation results. Firstly, Von Mises stress was employed to assess the risk of bone fracture. Secondly, relative micromotion between the prosthesis and the bone was used to assess the initial stability of the uncemented prosthesis. Micromotion was calculated by determining the relative displacement between two nodes: one on the prosthesis contact surface, and the other on the bone contact surface nearest to the former node. This computation was executed using an in-house Python script. Alongside the maximum micromotion value, “danger area” (the area of the contact surface where micromotion exceeded 40 μm) was also determined. Micromotion below 40 μm was considered beneficial for prosthesis stability.[40] Statistical analysis was carried out using SPSS v21.0 (IBM, USA). Paired *t*-tests were performed to compare the effects of ‘L = 1 mm’ versus ‘L = 5 mm’, and ‘gait’ versus ‘squat’ on both maximum Von Mises stress at the notch and maximum micromotion at the prosthesis-bone interface across all sagittal positions. A significance level of less than 0.05 was adopted.

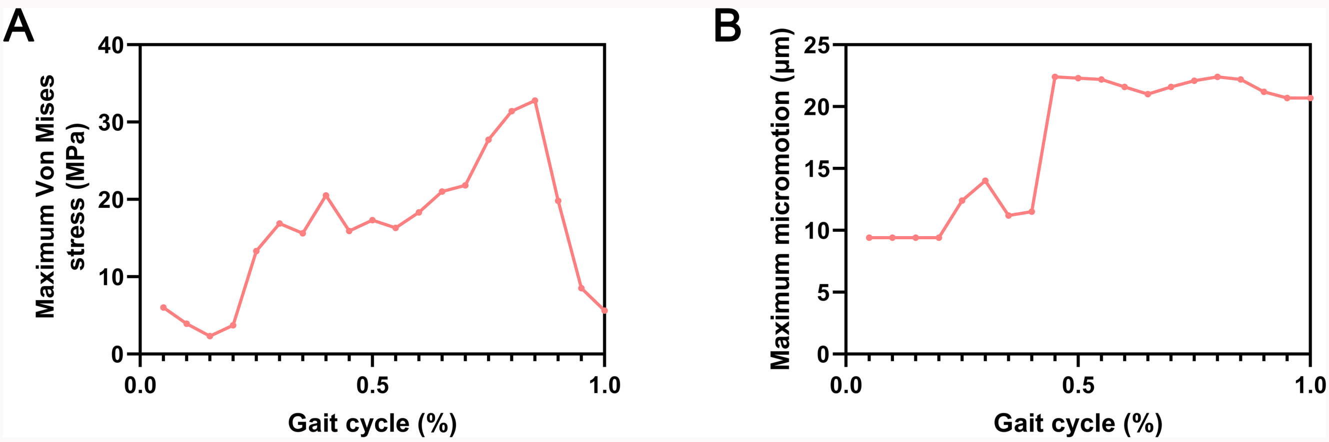

Fig. 5
The maximum a) Von Mises stress and b) micromotion change during the whole gait process when the sagittal positioning of the femoral component was -3 mm.

Table I. The maximum Von Mises stress at the notch and the maximum micromotion at the prosthesis-bone interface for all test conditions. Dashes signify that data were not available.

Sagittal position, mm	Maximum Von Mises stress, MPa				Maximum micromotion, µm			
	L = 1 mm		L = 5 mm		L = 1 mm		L = 5 mm	
	Gait	Squat	Gait	Squat	Gait	Squat	Gait	Squat
4	-	-	-	-	10.8	65.2	10.4	62.9
3	-	-	-	-	10.9	61.2	10.5	58.5
2	-	-	-	-	10	56.2	9.5	53.5
1	-	-	-	-	6.4	52.2	10	49.8
0	4.24	36.9	6.2	39.4	11.2	63.2	12.2	73.9
-1	9.59	49.3	10.3	51.1	13.7	81.3	13.7	83
-2	16.9	88.5	18.2	93	19.3	93.4	19.2	95.7
-3	24.7	128.3	28.2	143.3	24.1	103.4	22.4	106.1
-4	39.2	199.1	38.7	199.2	27.9	115.6	25.8	119.8
-5	48.8	242.5	48.6	225.1	30.6	128.4	29	137.3

Results

The maximum Von Mises stress and micromotion during the gait process

In this study, the entire gait process was simulated. As an example, the results of the -3 mm sagittal positioning (3 mm depth of femoral notch) are presented in this section. The maximum Von Mises stress at the femoral notch and the maximum micromotion are shown in Figure 5. The maximum Von Mises stress peaked at 85% of the gait, reaching 32.8 MPa. Concurrently, the maximum micromotion commenced at 45% of the gait and persisted throughout the second half of the gait, measuring 22.4 µm. The results of the other subgroups are provided in the third part of the Supplementary Material.

The Von Mises stress results of different femoral notching depths

Posterior positioning of the femoral component during TKA can lead to anterior notching of the femur, as depicted in Figure 1c. The Von Mises stress distribution of the notch is presented in Figure 6, and the maximum Von Mises stress results of varying femoral notching depths are presented in Figure 7 and Table I. It was observed that the maximum Von Mises stress increased with the deepening of the notch. For instance, with a notching depth of 3 mm and 'L' set at 1 mm, the maximum Von Mises stress was 24.7 MPa under gait condition and 128.3 MPa under squat condition, which increased 482.5% and 247.7%, respectively, compared to a notching depth of 0 mm. Von Mises stress levels were notably higher under squat condition than under the gait condition ($p = 0.001$, paired *t*-test). When the notch depth surpassed 3 mm, the maximum Von Mises stress exceeded 150 MPa under the squat condition. Interestingly, Von Mises stress results remained consistent regardless of whether 'L' was set at 1 mm or 5 mm, indicating no significant influence of the distance 'L' on notch Von Mises stress state ($p = 0.603$, paired *t*-test).

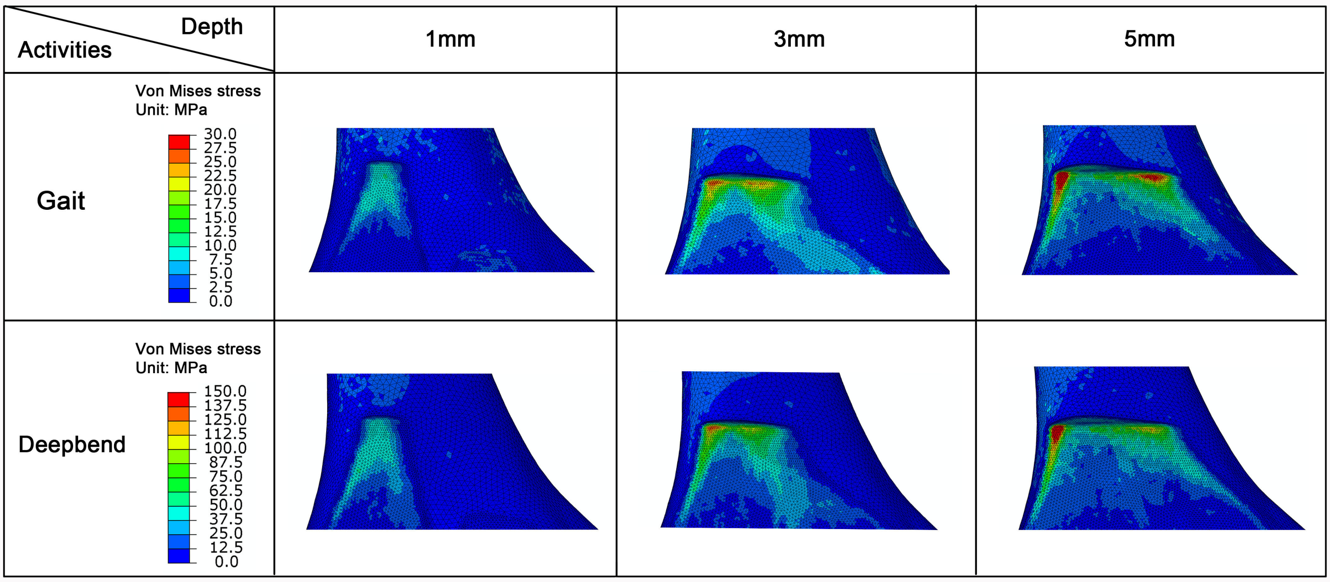

Fig. 6

The Von Mises stress distribution at the notching area when the notching depth was 1 mm, 3 mm, and 5 mm. The distance between the anterior flange of the femoral component and the notch (L) was 5 mm.

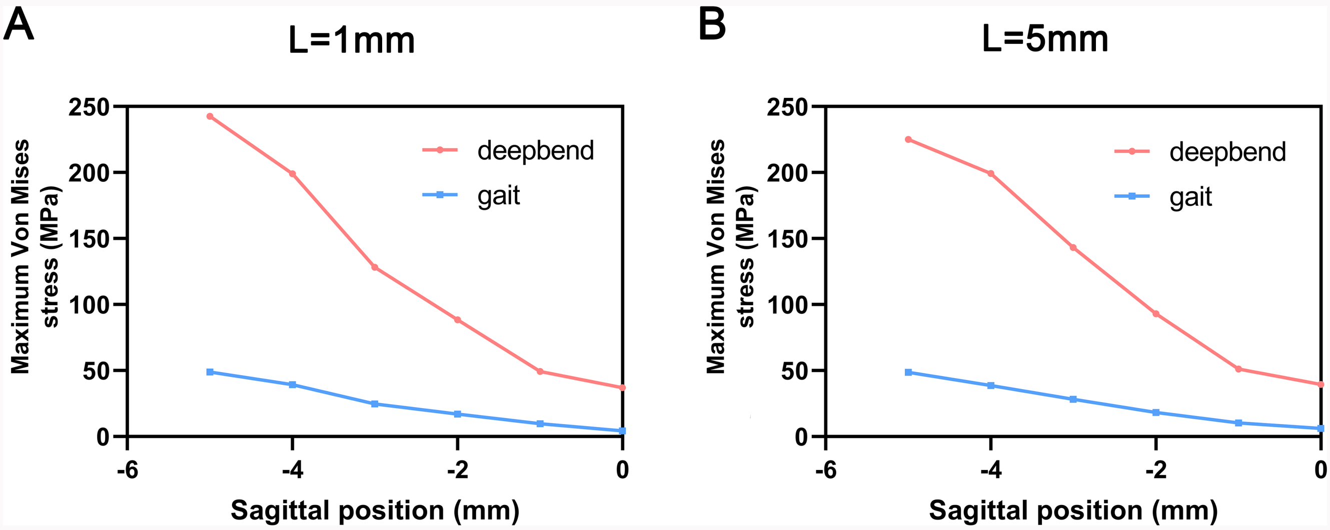

Fig. 7

The maximum Von Mises stress at different notching depths (sagittal positioning). The distance between the anterior flange of the femoral component and the notch (L) was a) 1 mm and b) 5 mm.

The micromotion results of different sagittal positioning of the femoral component

Figure 8 depicts the micromotion distribution at the femoral contact surface for sagittal positioning of -5 mm, 0 mm, and 4 mm. Notably, posterior positioning resulted in high micromotion at the anterior flange area, while anterior positioning led to high micromotion at the posterior condyle area.

The maximum micromotion for different sagittal positions of the femoral component is presented in Figure 9a and Table I. Under squat condition, the lowest maximum micromotion was recorded at 49.8 μm for a sagittal positioning of +1 mm, which was a slightly anterior positioning. Conversely, extremely anterior positioning (+4 mm) or posterior positioning (-5 mm) resulted in notably higher maximum micromotion, reaching 62.9 μm and 137.3 μm, respectively – marking increases of 26.3% and 175.7% compared to the +1 mm positioning.

The micromotion under gait condition followed a similar trend to the squat condition but was much lower ($p = 0.001$, paired *t*-test), with no micromotion exceeding 40 μm for all sagittal positions. Additionally, the results indicated no significant influence of the distance 'L' (set to 1 mm or 5 mm) on maximum micromotion or the danger area ($p = 0.285$ and 0.572, paired *t*-test).

For the squat condition, the contact surface area with micromotion exceeding 40 μm was calculated as the danger area (Figure 9b). Notably, the danger area was minimal (90.0 mm^2) at a sagittal position of 0 mm when 'L' was set to 1 mm, and similarly (85.5 mm^2) at a sagittal position of +1 mm when

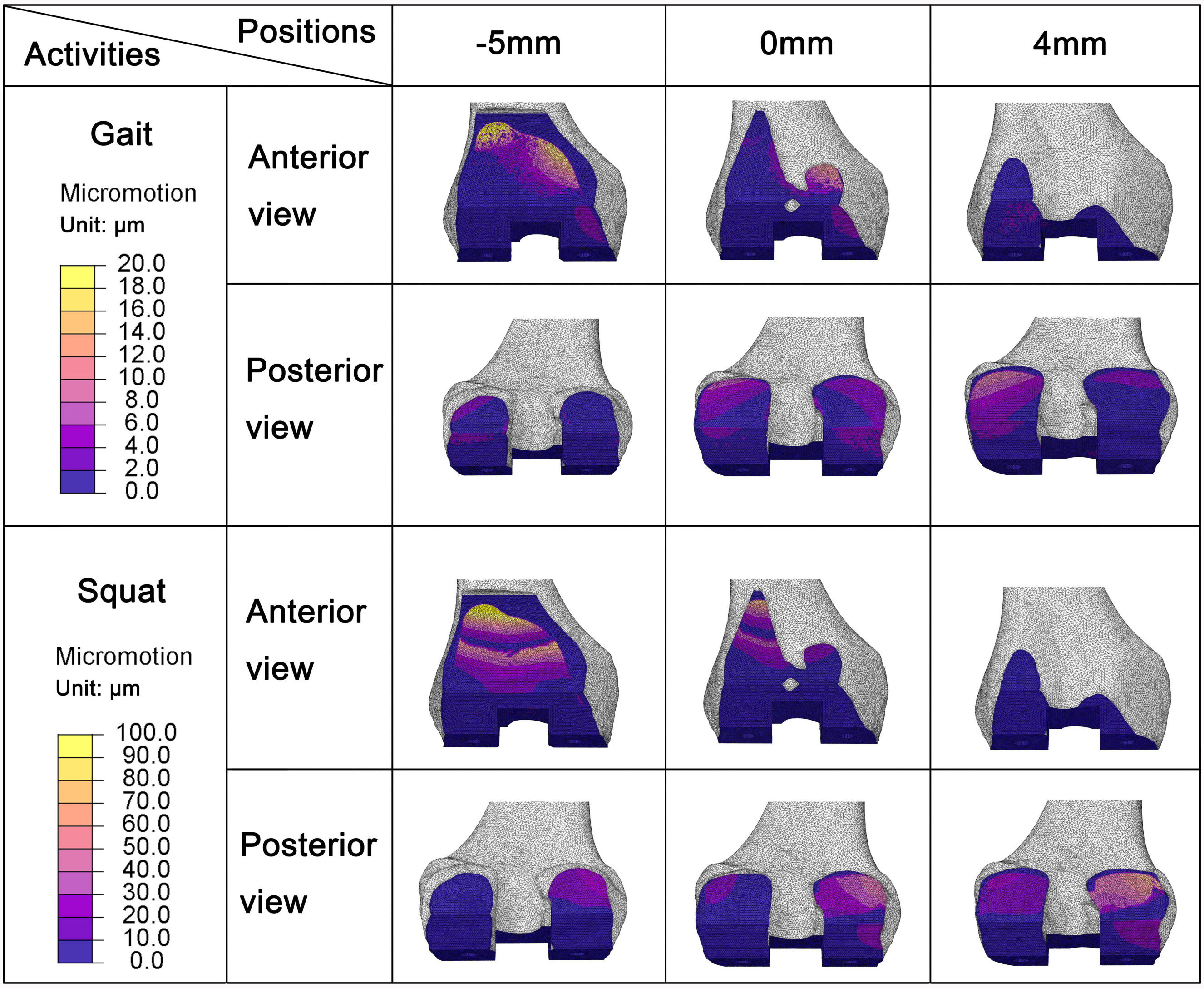

Fig. 8
Micromotion distribution at the femoral contact surface when the sagittal positioning of the femoral component was -5 mm, 0 mm, and 4 mm.

'L' was set to 5 mm. Extreme anterior or posterior positioning led to an expansion of the danger area.

Discussion

Periprosthetic fractures and aseptic loosening are the most common complications after knee arthroplasty, particularly among elderly patients.[41] The positioning of the femoral component has a profound effect on periprosthetic fractures and prosthetic loosening. Positioning in the coronal plane under navigation is now more precise. In contrast, there is no consensus on the optimal position and positioning method for the sagittal plane due to uncertainty of the reference point and anatomical differences in the patient. The effect of rotational positioning of the sagittal plane of the femoral prosthesis on joint kinematics and bone-prosthesis biomechanics has been studied in depth, while the effect of anterior-posterior positioning of the sagittal plane of the femoral prosthesis on periprosthetic fracture and aseptic loosening lacks research under physiological loading. In this study, we constructed an uncemented TKA model to investigate the risk of periprosthetic fracture and aseptic loosening of the prosthesis across various sagittal plane positions of the femoral component. We used Von Mises stress and interface micromotion as indicators under physiological loading conditions to assess these risks.

Von Mises stress was used to assess the risk of bone fracture in this study. Bone was considered susceptible to fracture if the Von Mises stress surpassed 150 MPa.[42] One of the most noteworthy findings was the notable increase in Von Mises stress at the notching area with deeper notches, with notching depths exceeding 3 mm posing a fracture risk (Figure 7). Particularly under squat condition, stress concentration at the notch area exceeded 150 MPa at sagittal positions of -4 mm and -5 mm, which could lead to the risk of periprosthetic femoral fracture. This is consistent with a previous meta-analysis study.[5] Furthermore, it was observed that when the notching depth exceeded 3 mm, stress concentration shifted away from the middle of the notch towards its sides (Figure 6). This occurred because full-thickness cortical bone was resected at the middle of the notch.[6,43] Consequently, the cortical bone on both sides of the notch experienced bending load, leading to pronounced stress concentration and a consequent reduction in femur bending strength, thereby elevating the risk of bone fracture. In light of these findings,

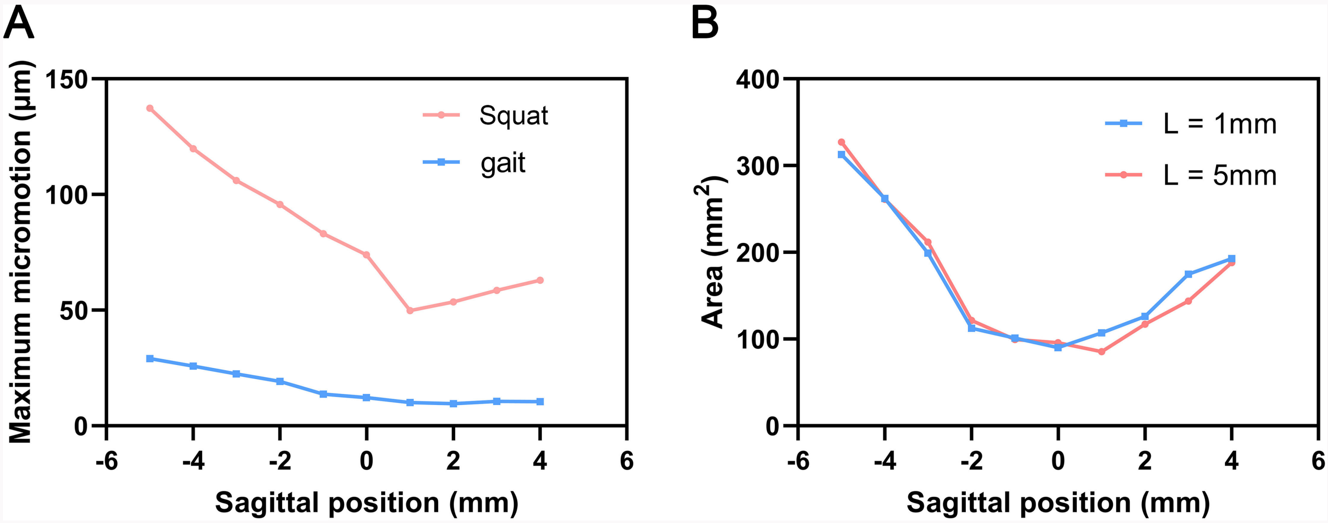

Fig. 9
a) Maximum micromotion (distance L = 5 mm) and b) danger area at different sagittal positioning.

surgeons facing intraoperative osteotomies with anterior femoral notches exceeding 3 mm may consider deploying salvage intramedullary stem to mitigate stress concentration at the notch. Prior research has indicated that a larger notching curvature correlates with reduced stress concentration,[43] suggesting that surgeons could potentially alleviate curvature by removing part of the cortical bone above the notch. This action would increase the distance 'L' between the notch and the anterior flange of the prosthesis. Notably, our study demonstrated that varying 'L' distances (1 mm and 5 mm) did not significantly influence stress at the notch ($p = 0.603$, paired *t*-test). Thus, easing the curvature of the notch emerges as a viable strategy to reduce the stress concentration and diminish the risk of periprosthetic femoral fracture.

The study findings highlighted a notable discrepancy in stress concentration between the squat and gait conditions, with the former exhibiting a 409.6% increase ($p = 0.001$, paired *t*-test) (Figure 7). Specifically, while Von Mises stress at the notch area remained below 50 MPa during gait conditions – significantly lower than the fracture-risk threshold of 150 MPa – squat loading conditions could escalate stress concentration beyond 150 MPa. This difference arises from the substantial reduction in distal femur bending strength induced by notching.[6,44] In contrast, the primary load during gait activity is vertical, and the Von Mises stress pattern at the notch under gait load closely resembles the vertical load pattern (Figures 4a and 5a). Fractures associated with femoral notching are more prone to occur within the initial three months postoperatively.[45] Consequently, it is advisable to perform gait exercises and minimize squat activity early postoperatively.

Aseptic loosening is one of the common complications after TKA. Excessive shear stress at the cemented prosthesis interface or excessive micromotion at the uncemented prosthesis interface are the causative factors for the development of aseptic loosening.[36] To elucidate the potential sites for aseptic loosening of the femoral component and evaluate the impact of sagittal positioning on prosthesis stability, the present study modelled the uncemented situation and analyzed the micromotion of the contact surface. Micromotion below 40 μm is believed to promote bone growth at the prosthesis-bone interface, while micromotion exceeding 150 μm can lead to fibrous tissue formation, compromising the stability of the prosthesis.[40,46] As depicted in Figure 8, when the femoral component was at a neutral sagittal position, the maximum micromotion occurred at the anterior flange area, consistent with previous findings.[36] Posterior positioning of the femoral component resulted in maximum micromotion at the anterior flange, increasing with further posterior positioning. This trend could be attributed to the high-stress concentration and deformation at the anterior notch. Conversely, anterior positioning of the femoral component led to maximum micromotion at the posterior condyle, increasing with further anterior positioning. It is worth noting that the maximum micromotion occurs in the posterior condyle at this time, probably because there is too little contact between the anterior flange and the bone for the micromotion analysis to capture the instability of the prosthetic anterior flange. In conditions where the prosthesis is placed too anteriorly, this is likely to lead to instability of the prosthesis. Excessive anterior or posterior positioning of the femoral component corresponded to heightened maximum micromotion.

Under the squat condition, the +1 mm sagittal positioning yielded the smallest maximum micromotion of 49.8 μm, which still exceeded the 40 μm threshold. The danger area was minimized at the relatively neutral sagittal position (0 mm sagittal position for L = 1 mm and +1 mm sagittal position for L = 5 mm), indicating that the neutral sagittal position (0 mm) or a slightly anterior position (+1 mm) was the proper sagittal position for the femoral component. Meanwhile, the maximum micromotion under gait condition was significantly lower compared to squat condition (80.3% lower; $p = 0.001$, paired *t*-test), remaining below 40 μm across all tested sagittal positions. This suggests that certain gait exercises would not compromise postoperative femoral component stability. Appropriate mechanical stimulation and low-level micromotion could benefit the second biological fixation induced by bone formation.[47] Additionally, postoperative intermittent parathyroid hormone has been shown to enhance stability and osseointegration of initially unstable prostheses, warranting consideration for early postoperative use.[48] However, it is not recommended to engage in squat activities during the early postoperative period, as high interface micromotion can compromise femoral component stability and increase the risk of aseptic loosening.

Undoubtedly, the impact of prosthesis positioning on the musculoskeletal system is multifaceted, and this study focused solely on femur and femoral prostheses without considering the altered kinematics and mechanical environment resulting from anterior and posterior femoral component positioning. Notably, posterior placement of the femoral component has been associated with enhanced quadriceps strength, reduced patellofemoral contact stress, and alleviated pain and wear on the anterior knee aspect. Furthermore, such positioning results in a decreased flexion gap.[49] However, beyond sagittal plane positioning, the flexion-extension and rotational positioning of the femoral component significantly influence postoperative outcomes. Extension positioning increases the risk of anterior femoral notching, whereas flexion positioning enhances quadriceps muscle strength and diminishes patellofemoral stress. Nonetheless, excessive flexion positioning may lead to tibial column and femoral prosthesis impingement, thereby limiting knee flexion clearance.[50] Presently, positioning perpendicular to the distal femur anterior cortex axis – approximately 3° to 5° of flexion relative to the femoral mechanical axis – is deemed optimal for flexion-extension positioning of the femoral component.[29,51] Integrating the findings of this study, which suggest that the optimal sagittal positioning of the femoral component is neutral (0 mm, flush with the distal femur anterior cortex axis) or slightly anterior (+1 mm), provides a comprehensive understanding of appropriate femoral component sagittal positioning.

This study has several limitations that warrant acknowledgement. First, the modelling focused solely on the femur and femoral prostheses, thereby neglecting the impact of prosthesis positioning on joint space and kinematics. Incorporating these factors would offer a more comprehensive understanding of the overall biomechanical effects. Second, biomechanical validations were conducted using synthetic femora, which possess material properties distinct from real bone. Future endeavours should strive to employ cadaveric bone for both finite element modelling and mechanical experimentation to better reflect real-world conditions. Moreover, individualized modelling introduces potential sampling errors, and the influence of variables such as sex and age was not accounted for. Utilizing computer algorithms to generate generic models based on extensive CT data may mitigate sampling errors associated with individual modelling in future studies. Lastly, this study did not delve into the influence of femoral rotation or consider cruciate-retaining and cemented TKA scenarios. While incorporating these factors would undoubtedly enrich the analysis, the sheer volume of resulting data poses challenges in presenting comprehensive findings within a single article. Nonetheless, these aspects will be explored in subsequent investigations. While this study focuses on the uncemented situation, its findings can still offer insights applicable to the cemented scenario, given the informative nature of the results.

The findings of this study highlight the significance of sagittal positioning in mitigating the risk of aseptic loosening and periprosthetic femoral fracture. Specifically, a neutral sagittal position (0 mm) or a slightly anterior position (+1 mm) of the femoral component emerged as favourable choices. These positions effectively alleviate stress concentration at the femoral notching site and minimize interface micromotion, thus enhancing the stability and longevity of the prosthesis. By adopting such sagittal positioning strategies, orthopaedic surgeons can potentially reduce the incidence of complications associated with total knee arthroplasty, ultimately improving patient outcomes and quality of life.

Supplementary material

Method and results of the model validation, method and results of the mesh sensitivity analysis, results of the maximum Von Mises stresses and micromotion for each group, and results of the maximum principal stress distribution for each group.

References

1. **Santini AJA**, **Raut V**. Ten-year survival analysis of the PFC total knee arthroplasty--a surgeon's first 99 replacements. *Int Orthop*. 2008;32(4):459–465.
2. **Cheung A**, **Goh SK**, **Tang A**, **Keng TB**. Complications of total knee arthroplasty. *Current Orthopaedics*. 2008;22(4):274–283.
3. **Delanois RE**, **Mistry JB**, **Gwam CU**, **Mohamed NS**, **Choksi US**, **Mont MA**. Current epidemiology of revision total knee arthroplasty in the United States. *J Arthroplasty*. 2017;32(9):2663–2668.
4. **Dagneaux L**, **Amundson AW**, **Larson DR**, **Pagnano MW**, **Berry DJ**, **Abdel MP**. Contemporary mortality rate and outcomes in nonagenarians after aseptic revision hip and knee arthroplasty. *Bone Joint J*. 2023;105-B(6):649–656.
5. **Stamiris D**, **Gkekas NK**, **Asteriadis K**, **et al**. Anterior femoral notching ≥3mm is associated with increased risk for supracondylar periprosthetic femoral fracture after total knee arthroplasty: a systematic review and meta-analysis. *Eur J Orthop Surg Traumatol*. 2022;32(3):383–393.
6. **Lesh ML**, **Schneider DJ**, **Deol G**, **Davis B**, **Jacobs CR**, **Pellegrini VD**. The consequences of anterior femoral notching in total knee arthroplasty. A biomechanical study. *J Bone Joint Surg Am*. 2000;82-A(8):1096–1101.
7. **Zainul-Abidin S**, **Lim B**, **Bin-Abd-Razak HR**, **et al**. Periprosthetic fractures after total knee arthroplasty: the influence of pre-operative mechanical factors versus intraoperative factors. *Malays Orthop J*. 2019;13(2):28–34.
8. **Su WL**, **You KD**, **Yang CC**, **Wu JJ**, **Yeh MK**. Stress analysis of improper femur cut in total knee arthroplasty by finite element method. *Journal of Mechanics*. 2020;36(3):315–322.
9. **Chowdhry M**, **Bamne AB**, **Na YG**, **Kang YG**, **Kim TK**. Prevalence and predictors of post-operative coronal alignment outliers and their association with the functional outcomes in navigated total knee arthroplasty. *J Arthroplasty*. 2014;29(12):2357–2362.
10. **Fu Y**, **Wang M**, **Liu Y**, **Fu Q**. Alignment outcomes in navigated total knee arthroplasty: a meta-analysis. *Knee Surg Sports Traumatol Arthrosc*. 2012;20(6):1075–1082.
11. **Alazzawi S**, **Field MH**, **Bardakos NV**, **Freeman MAR**, **Field RE**. The position of the centre of the femoral head relative to the midline of the pelvis: a consistent landmark in total knee replacement surgery. *Knee*. 2012;19(6):827–831.
12. **Huang G**, **Xia J**, **Wang S**, **et al**. Total knee arthroplasty using trochlear groove as guide for position of femoral component in severe knee osteoarthritis. *BMC Surg*. 2016;16(1):33.
13. **Burnett RSJ**, **Barrack RL**. Computer-assisted total knee arthroplasty is currently of no proven clinical benefit: a systematic review. *Clin Orthop Relat Res*. 2013;471(1):264–276.
14. **Lee JH**, **Wang S-I**. Risk of anterior femoral notching in navigated total knee arthroplasty. *Clin Orthop Surg*. 2015;7(2):217–224.

15. **Completo A**, **Fonseca F**, **Relvas C**, **Ramos A**, **Simões JA**. Improved stability with intramedullary stem after anterior femoral notching in total knee arthroplasty. *Knee Surg Sports Traumatol Arthrosc*. 2012;20(3):487–494.
16. **Ritter MA**, **Thong AE**, **Keating EM**, **et al**. The effect of femoral notching during total knee arthroplasty on the prevalence of postoperative femoral fractures and on clinical outcome. *J Bone Joint Surg Am*. 2005;87-A(11):2411–2414.
17. **Minarro JC**, **Urbano-Luque MT**, **López-Jordán A**, **López-Pulido MJ**, **González-Fernández Á**, **Delgado-Martínez AD**. Is the fracture pattern in periprosthetic fractures around the knee related with the anterior femoral notch? *J Clin Orthop Trauma*. 2018;9(4):289–291.
18. **Lombardi Jr AV**, **Berend KR**, **Adams JB**. Why knee replacements fail in 2013: patient, surgeon, or implant? *Bone Joint J*. 2014;96-B(11_Supple_A):101–104.
19. **Gao F**, **Henricson A**, **Nilsson KG**. Cemented versus uncemented fixation of the femoral component of the NexGen CR total knee replacement in patients younger than 60 years: a prospective randomised controlled RSA study. *Knee*. 2009;16(3):200–206.
20. **Nilsson KG**, **Henricson A**, **Norgren B**, **Dalén T**. Uncemented HA-coated implant is the optimum fixation for TKA in the young patient. *Clin Orthop Relat Res*. 2006;448:129–139.
21. **Brown TE**, **Harper BL**, **Bjorgul K**. Comparison of cemented and uncemented fixation in total knee arthroplasty. *Orthopedics*. 2013;36(5):380–387.
22. **Kurtz SM**, **Lau E**, **Ong K**, **Zhao K**, **Kelly M**, **Bozic KJ**. Future young patient demand for primary and revision joint replacement: national projections from 2010 to 2030. *Clin Orthop Relat Res*. 2009;467(10):2606–2612.
23. **Nojiri S**, **Hayakawa K**, **Date H**, **et al**. Which is better? Anterior or posterior referencing for femoral component position in total knee arthroplasty. *J Orthop Surg (Hong Kong)*. 2021;29(1):23094990211002325.
24. **Kreuzer SW**, **Pourmoghaddam A**, **Leffers KJ**, **Johnson CW**, **Dettmer M**. Computed tomography analysis of postsurgery femoral component rotation based on a force sensing device method versus hypothetical rotational alignment based on anatomical landmark methods: a pilot study. *Adv Orthop*. 2016;2016:4961846.
25. **Conlisk N**, **Howie CR**, **Pankaj P**. Computational modelling of motion at the bone-implant interface after total knee arthroplasty: the role of implant design and surgical fit. *Knee*. 2017;24(5):994–1005.
26. **Completo A**, **Simões JA**, **Fonseca F**. Revision total knee arthroplasty: the influence of femoral stems in load sharing and stability. *Knee*. 2009;16(4):275–279.
27. **Conlisk N**, **Gray H**, **Pankaj P**, **Howie CR**. The influence of stem length and fixation on initial femoral component stability in revision total knee replacement. *Bone Joint Res*. 2012;1(11):281–288.
28. **Completo A**, **Fonseca F**, **Simões JA**. Experimental validation of intact and implanted distal femur finite element models. *J Biomech*. 2007;40(11):2467–2476.
29. **Kanna R**, **Ravichandran C**, **Shetty GM**. Notching is less, if femoral component sagittal positioning is planned perpendicular to distal femur anterior cortex axis, in navigated TKA. *Knee Surg Relat Res*. 2021;33(1):46.
30. **Mo F**, **Zhang H**, **Zhao S**, **Xiao Z**, **Liu T**. Coupling musculoskeletal dynamics and subject-specific finite element analysis of femoral cortical bone failure after endoprosthetic knee replacement. *Appl Bionics Biomech*. 2019;2019:4650405.
31. **Zhang A**, **Chen H**, **Liu Y**, **et al**. Customized reconstructive prosthesis design based on topological optimization to treat severe proximal tibia defect. *Bio-Design and Manufacturing*. 2021;4(1):87–99.
32. **Somovilla-Gómez F**, **Lostado-Lorza R**, **Corral-Bobadilla M**, **Escribano-García R**. Improvement in determining the risk of damage to the human lumbar functional spinal unit considering age, height, weight and sex using a combination of FEM and RSM. *Biomech Model Mechanobiol*. 2020;19(1):351–387.
33. **Liu Y**, **Zhang A**, **Wang C**, **et al**. Biomechanical comparison between metal block and cement-screw techniques for the treatment of tibial bone defects in total knee arthroplasty based on finite element analysis. *Comput Biol Med*. 2020;125:104006.
34. **Kutzner I**, **Heinlein B**, **Graichen F**, **et al**. Loading of the knee joint during activities of daily living measured in vivo in five subjects. *J Biomech*. 2010;43(11):2164–2173.
35. **Zelle J**, **van de Groes SAW**, **de Waal Malefijt MC**, **Verdonschot N**. Femoral loosening of high-flexion total knee arthroplasty: the effect of posterior cruciate ligament retention and bone quality reduction. *Med Eng Phys*. 2014;36(3):318–324.
36. **Berahmani S**, **Janssen D**, **Wolfson D**, **et al**. FE analysis of the effects of simplifications in experimental testing on micromotions of uncemented femoral knee implants. *J Orthop Res*. 2016;34(5):812–819.
37. **Conlisk N**, **Howie CR**, **Pankaj P**. The role of complex clinical scenarios in the failure of modular components following revision total knee arthroplasty: a finite element study. *J Orthop Res*. 2015;33(8):1134–1141.
38. **Liu Y**, **Chen B**, **Wang C**, **et al**. Design of porous metal block augmentation to treat tibial bone defects in total knee arthroplasty based on topology optimization. *Front Bioeng Biotechnol*. 2021;9:765438.
39. **Taylor M**, **Barrett DS**, **Deffenbaugh D**. Influence of loading and activity on the primary stability of cementless tibial trays. *J Orthop Res*. 2012;30(9):1362–1368.
40. **Vandamme K**, **Naert I**, **Geris L**, **Vander Sloten J**, **Puers R**, **Duyck J**. The effect of micro-motion on the tissue response around immediately loaded roughened titanium implants in the rabbit. *Eur J Oral Sci*. 2007;115(1):21–29.
41. **COMPOSE Study Team**. Epidemiology and characteristics of femoral periprosthetic fractures: data from the characteristics, outcomes and management of periprosthetic fracture service evaluation (COMPOSE) cohort study. *Bone Joint J*. 2022;104-B(8):987–996.
42. **Reilly DT**, **Burstein AH**. The elastic and ultimate properties of compact bone tissue. *J Biomech*. 1975;8(6):393–405.
43. **Zalzal P**, **Backstein D**, **Gross AE**, **Papini M**. Notching of the anterior femoral cortex during total knee arthroplasty characteristics that increase local stresses. *J Arthroplasty*. 2006;21(5):737–743.
44. **Shawen SB**, **Belmont PJ**, **Klemme WR**, **Topoleski LDT**, **Xenos JS**, **Orchowski JR**. Osteoporosis and anterior femoral notching in periprosthetic supracondylar femoral fractures: a biomechanical analysis. *J Bone Joint Surg Am*. 2003;85-A(1):115–121.
45. **Fokin AA**, **Heekin RD**. Anterior referencing versus posterior referencing in total knee arthroplasty. *J Knee Surg*. 2014;27(4):303–308.
46. **Pilliar RM**, **Lee JM**, **Maniatopoulos C**. Observations on the effect of movement on bone ingrowth into porous-surfaced implants. *Clin Orthop Relat Res*. 1986;208:108–113.
47. **Suárez DR**, **Nerkens W**, **Valstar ER**, **Rozing PM**, **van Keulen F**. Interface micromotions increase with less-conforming cementless glenoid components. *J Shoulder Elbow Surg*. 2012;21(4):474–482.
48. **Staats K**, **Sosa BR**, **Kuyl E-V**, **et al**. Intermittent parathyroid hormone increases stability and improves osseointegration of initially unstable implants. *Bone Joint Res*. 2022;11(5):260–269.
49. **Puranik HG**, **Mukartihal R**, **Patil SS**, **Dhanasekaran SR**, **Menon VK**. Does femoral notching during total knee arthroplasty influence periprosthetic fracture. A prospective study. *J Arthroplasty*. 2019;34(6):1244–1249.
50. **Okamoto Y**, **Otsuki S**, **Nakajima M**, **Jotoku T**, **Wakama H**, **Neo M**. Sagittal alignment of the femoral component and patient height are associated with persisting flexion contracture after primary total knee arthroplasty. *J Arthroplasty*. 2019;34(7):1476–1482.
51. **Nishitani K**, **Kuriyama S**, **Nakamura S**, **et al**. Excessive flexed position of the femoral component causes abnormal kinematics and joint contact/ ligament forces in total knee arthroplasty. *Sci Rep*. 2023;13(1):6356.

Author information

Q. Wan, PhD, Orthopaedic Surgeon
Q. Han, PhD, Professor
Y. Liu, PhD, Orthopaedic Surgeon
H. Chen, PhD, Orthopaedic Surgeon
A. Zhang, PhD, Orthopaedic Surgeon
J. Wang, PhD, Professor
Department of Orthopedics, The Second Hospital of Jilin University, Changchun, China.

X. Zhao, PhD, Orthopaedic Surgeon, Department of Endocrinology and Metabolism, The First Hospital of Jilin University, Changchun, China.

Author contributions

Q. Wan: Investigation, Methodology, Visualization, Writing – original draft, Writing – review & editing.
Q. Han: Conceptualization, Funding acquisition, Project administration, Resources, Supervision, Validation, Writing – review & editing.
Y. Liu: Investigation, Methodology, Supervision, Validation, Visualization, Writing – review & editing.
H. Chen: Software, Validation, Writing – review & editing.
A. Zhang: Software, Validation, Writing – review & editing.
X. Zhao: Project administration, Investigation.
J. Wang: Conceptualization, Funding acquisition, Project administration, Resources, Supervision, Validation.

Q. Wan and Q. Han contributed equally to this work.

Q. Wan and Q. Han are joint first authors.

Funding statement

The authors disclose receipt of the following financial or material support for the research, authorship, and/or publication of this article: 1) National Natural Science Foundation of China (grant numbers 82072456 & 81802174); 2) Department of Science and Technology of Jilin Province, P.R.C. (grant numbers 20200404202YY, 220200201453JC, YDZJ202301ZYTS076, & 20210101439JC); 3) Department of Finance in Jilin Province (grant number 2020SCZT037); 4) Interdisciplinary Integration and Cultivation Project of Jilin University (grant number JLUXKJC2020307); 5) The First Hospital of Jilin University (JDYYCB-2023010); and 6) The Central University Basic Scientific Research Fund (2023-JCXK-04).

ICMJE COI statement

Q. Han reports institutional payments from: the National Natural Science Foundation of China (grant numbers 82072456 & 81802174); Department of Science and Technology of Jilin Province, P.R.C. (grant number 220200201453JC); Department of Finance in Jilin Province (grant number 2020SCZT037); and Interdisciplinary Integration and Cultivation Project of Jilin University (grant number JLUXKJC2020307). X. Zhao reports institutional payments from the Department of Science and Technology of Jilin Province, P.R.C. (grant number 20210101439JC) and The First Hospital of Jilin University (JDYYCB-2023010). Y. Liu reports an institutional payment from The Central University Basic Scientific Research Fund (2023-JCXK-04). J. Wang reports an institutional payment from the Department of Science and Technology of Jilin Province, P.R.C. (grant number 20200404202YY). A. Zhang reports an institutional payment from the Department of Science and Technology of Jilin Province, P.R.C. (grant number YDZJ202301ZYTS076).

Data sharing

The data that support the findings for this study are available to other researchers from the corresponding author upon reasonable request.

Ethical review statement

This study was performed in line with the principles of the Declaration of Helsinki. Approval was granted by the Ethics Committee of the Second Hospital of Jilin University.

Open access funding

The open access publication of this article was self-funded.